International Journal of Naval Architecture and Ocean Engineering 11 (2019) 858–864

Contents lists available at ScienceDirect

International Journal of Naval Architecture and Ocean Engineering

journal homepage: http://www.journals.elsevier.com/international-journal-of-naval-architecture-and-ocean-engineering/

Influence on properties of base metal after elimination of lifting-lug member in a dissimilar welding between steel base and steel lifting lug

Jeongung Park [a], Gyubaek An [b, *], Haewoo Lee [c]

[a] Dept. of Civil Engineering, Chosun University, South Korea
[b] Dept. of Naval Architecture and Ocean Engineering, Chosun University, South Korea
[c] Dept. of Material Science and Engineering, Dong-A University, South Korea

ARTICLE INFO

Article history:
Received 14 November 2018
Received in revised form
25 February 2019
Accepted 16 April 2019
Available online 27 April 2019

Keywords:
Lifting lugs
Metal microstructure
Shipbuilding
Offshore construction
Emission spectrochemical analysis
Dissimilar welding

ABSTRACT

The increasing demands of lifting lugs can be attributed to the rapid advancement of shipbuilding and offshore-structure production technologies and an exponential increase in the size of the block units of ship structures. Therefore, to ensure safety during the transportation and turnover of large blocks, it is important to determine the structural integrity and position of lifting lugs. However, because the manufacturing cost and availability of lugs are important considerations, low cost and easily obtainable steel compositions of grades different from those of the blocks are often used as alternatives. The purpose of this study is to investigate the effect of a lifting-lug metal on the physical properties of a base metal in a dissimilar welding between the base metal and lifting lug. The effect was evaluated by observing the metal microstructures and determining the hardness and dilution values on the cross-sectional surface of the lifting lug. According to the results of the metal microstructures, impact, hardness, and emission spectrochemical analysis at the surface from where the lug was removed confirmed that the chemical composition of the lifting-lug metal did not influence the physical properties of the base metal.

1. Introduction

Block transportation and turnover are essential operations in shipbuilding and offshore construction processes (ASME, 2008). These processes use a large number of lifting lug members to perform the block transportation and turnover operations. In the recent years, the demand for lifting lugs has increased in various fields, such as in the installation and mooring of floating offshore wind turbines. The reasons for this increase include the rapid advancement of shipbuilding and offshore-structure production technologies and an exponential increase in the size of the block units of ship structures. Therefore, to ensure safety during the transportation and turnover of large blocks, it is important to determine the structural integrity and position of lifting lugs. However, because the manufacturing cost and availability of lugs are important considerations, low cost and easily obtainable steel compositions of grades different from those of the blocks are often used as alternatives. If the steel used in lifting lugs is of a grade lower than that used in the base, the lug steel will meld into the base steel and change the chemical composition of the latter. Particularly, when a marine structure is manufactured using steel at a low temperature (An et al., 2017; Hoshino et al., 2004), dilution by welding using dissimilar steel plates that can be easily used at the factory may affect the safety of the welded steel structure. These safety issues arise when the lifting lug breaks owing to the inadequate engineering design developed for reducing cost, or weakens in strength owing to its composition being different from that of the payload it carries. Therefore, the focus should shift to developing an optimal design (Kim, 2006).

Several research studies have been conducted to reduce the manufacturing cost and improve the rational design of lifting lugs. However, using this structural rationalization study (Ham, 2001) to present a desirable and improved structure has proven difficult for engineers owing to the lack of an optimization theory and experience. To overcome this difficulty, a hybrid structural design system

* Corresponding author.
E-mail address: gyubaekan@chosun.ac.kr (G. An).
Peer review under responsibility of Society of Naval Architects of Korea.

https://doi.org/10.1016/j.ijnaoe.2019.04.003

(Kim et al., 1998; Ham et al., 2009; Ham, 2011) that can produce optimal profiles for and simultaneously examine the strength of specific types of lifting lugs was developed. This system made it possible to obtain an optimal design by deriving an optimal shape, design a lightweight lifting lug with a high turn ratio using the strength formula, and perform structural analysis using the Finite Element Method (FEM). The improved lifting lug obtained through this system can help in increasing the reuse frequency and has an advantage over other lugs in terms of strength (Kim, 2003).

When welded using readily available steel grades for cost reduction, the lifting lugs dilute into the welds, which may affect the strength of the actual structure. Nouri et al. (2007) conducted a study on the effect of gas metal arc welding conditions in pipe cladding on the dilution and weld bead shapes of lifting lugs. The study found that higher the welding wire feed rate is, more is the dilution and bead height and width; however, the welding speed decreased. Om et al. (2013) and Gunaraja and Murugan (1999) investigated the effect of Submerged Arc Welding (SAW) polarity and weld parameters on the size and dilution properties of Heat Affected Zones (HAZs). The width and area of HAZs increased linearly with the input heat, irrespective of the electrical polarity. In addition, Kim et al. (1996) studied the effects of linear cracks on real structures using Magnetic Particle Inspection (MPI) after the removal of lug by oxygen/ethylene flame. According to their results, the welding slag penetrated into the metal base instead of penetrating into the diluted metal of the lug. Several research studies on the structural safety of the lifting lug member have been performed. However, there has been little research on the effect of the dilution by dissimilar welding from the low-grade lifting lugs to the high-grade base steel in dissimilar welding.

The purpose of this study is to investigate the effect of lifting-lug metal on the physical properties of the base metal in a dissimilar welding between the two. The effect was evaluated by observing the metal microstructures and determining the hardness and dilution values on the cross-sectional surface of the lifting lug.

2. Specimen preparation

Fig. 1 shows the shape and dimensions of the fillet-welded specimen used in the experiment. The base metals used were B-grade and EH36 shipbuilding steel, and the lifting lug metals were A-grade steel and marine-grade stainless steel (STS) 316L. The base metal was 200 mm wide and 150 mm length. The thicknesses of the B-grade, EH36, A-grade, and STS316L steels were 20, 30, 20, and 10 mm, respectively. For a lifting lug thickness of 20 mm, a groove of 40° was made and full penetration welding was performed, while for a lug thickness of 10 mm, fillet welding was performed. The types of steel and welding wires used are listed in Table 1, and the welding conditions are listed in Table 2. Flux Core Arc (FCA) welding was performed on the lugs, and the welding wire was selected according to the grades of the two steel types that were welded. Fig. 2 shows an image of the fillet-welded specimen.

Table 1
Specimens grade and consumable wire.

Test No.	Base Metal (grade)	Lifting Lug Metal (grade)	Consumable wire
F1	B	A(SS400)	SC-71LH
F2	EH36	A(SS400)	DS II-81-K2
F3	B	STS 316 L	SB309MOL
F4	EH36	STS 316 L	SB309MOL

Table 2
Welding conditions.

Test No.	Current(A)	Voltage(V)	Travel speed (cm/s)
F1, F2	260	25	40
F3,F4	240	25	40

Fig. 3 shows the cross section of the welded structure and location on the test specimens to observe the metal microstructures and measure the hardness and dilution values. In Fig. 3(a), the lifting lug is cut at the top of the weld bead using a saw. In Fig. 3(c), the remaining beads are grounded until the height of the welds is equal to that of the surface of the base. The test specimen was sampled at the center of the base metal from where the beads were grounded and removed. Fig. 4 shows the surface and cross section of the specimen taken from the welded structure.

3. Results and discussion

3.1. Metal microstructures

Mounting, polishing, and etching operations were required to inspect the metal microstructures of the base metal from where the lifting lugs were removed. A resin and hardener were mixed and placed in a frame with a sample and subsequently hardened. The mounted specimens were then polished using rough and soft sandpapers consecutively. The surface of the test specimen was corroded using nitric acid and alcohol. The metal microstructures of the corroded specimen were then observed using an optical microscope of 200× magnification. Figs. 5–8 show the metal microstructures of the test specimens F1, F2, F3, and F4, respectively. The observation positions for each of the specimens are at the weld metal, fusion line (F/L), 1 mm position from fusion line (F/L + 1), and 2 mm position (F/L + 2). The base metal of specimens F1 and F3 were made of B-grade steel, while those of specimens F2 and F4 were made of EH36 steel. The lifting lugs of specimens F1 and F2 were made of SS400 steel, while those of specimens F3 and F4 were made of STS316L. The microstructure of the weld deposit metal is determined by the welding wire and heat input. Figs. 5 and 6 show

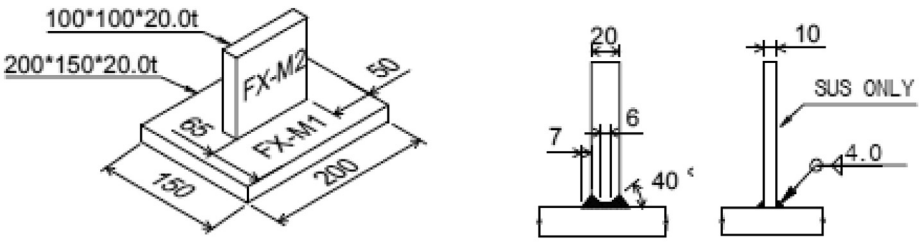

(a) Specimen shape (b) Groove Shape

Fig. 1. Shape of specimens and groove.

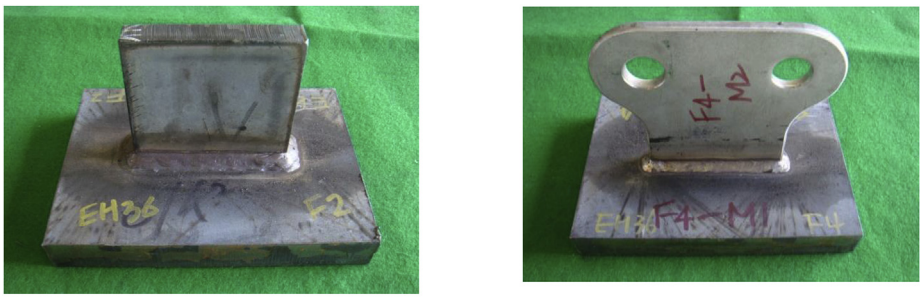

(a)Specimens F1, F2 (b) Specimens F3, F4

Fig. 2. Specimen pictures.

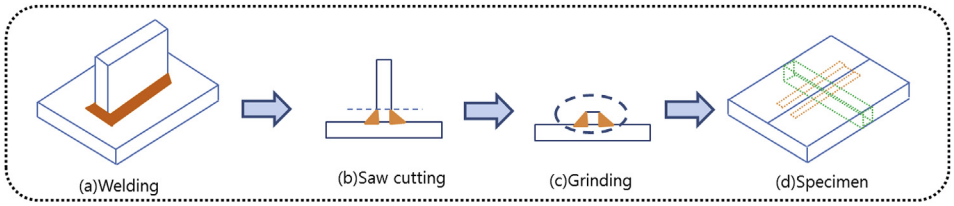

Fig. 3. Process of cutting specimens from welded structure.

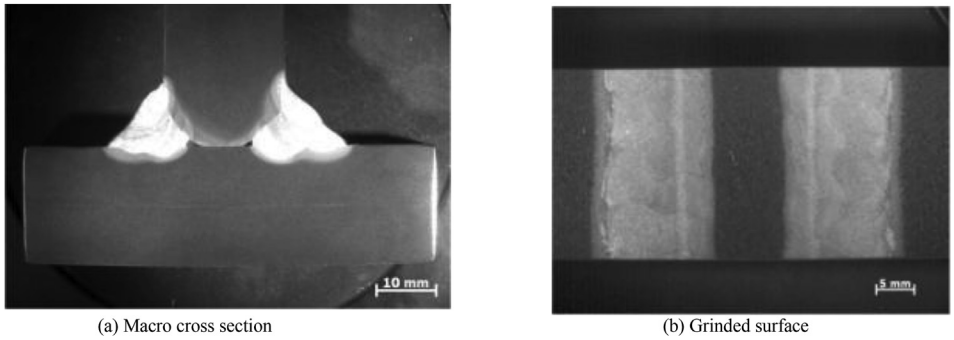

(a) Macro cross section (b) Grinded surface

Fig. 4. Macro cross section and grinded base surface (No. F1).

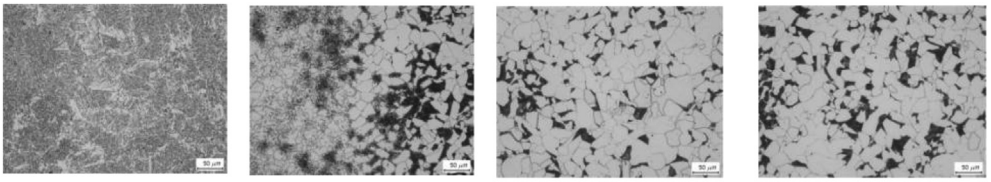

(a) WM (b) F/L (c) F/L+1 (d) F/L+2

Fig. 5. Micro structure of grinded base metal surface in F1 specimens.

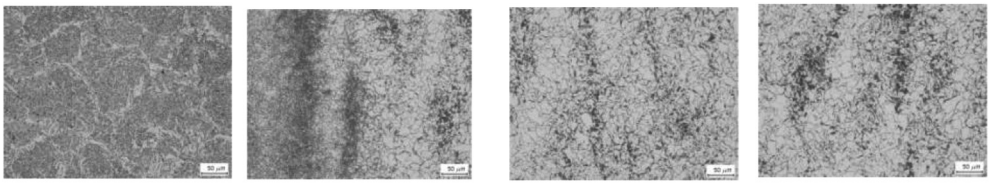

(a) WM (b) F/L (c) F/L+1 (d) F/L+2

Fig. 6. Micro structure of grinded base metal surface in F2 specimens.

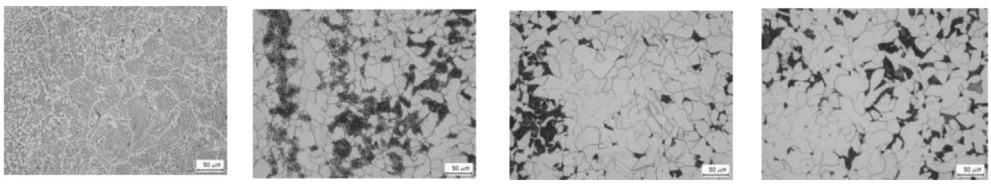

Fig. 7. Micro structure of grinded base metal surface in F3 specimens.

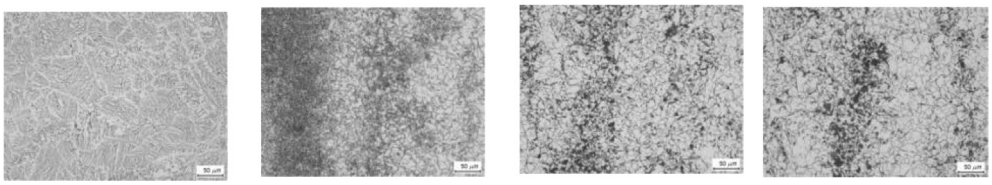

Fig. 8. Micro structure of grinded base metal surface in F4 specimens.

that both the base and lifting lug are made of carbon steel, which is composed of grain-bound ferrite and acicular ferrite. When the temperature exceeds 1300 °C in the fusion line, the crystal grains become coarse and cause a decrease in toughness (Welding handbook, 1991). The rate of growth of the grains in HAZs depends on the input heat, thickness of the base metal, etc. An HAZ is classified into a crystal grain coarsening region at 1300 °C or more and a grain-refining region near the A3 transformation temperature depending on the heating temperature. The crystal grain region in the HAZ is heated at a temperature close to the solidus temperature and cooled rapidly to enable the extraction of carbides and nitrides. In the case of the austenitic stainless steel (STS316L), the austenite phase formed after solidification persists without a phase transformation at room temperature; however, in the case of the carbon steel, many phase changes occur during the cooling process. Except at the part of the welding metal, similar metal structures were observed at all other observation positions depending on the characteristics of the base metal. Therefore, the results of the metallurgical process at the welds showed a metallic texture similar to that of the welding wire. This is because the welding wire was selected by the better quality metal component of the two weld metals. Cellular or dendrite coagulation types are observed in the melting zone of the weld, planar coagulation is observed near the fusion line where the temperature gradient is large and the growth rate is slow, and equiaxed dendrite coagulation is observed where the temperature gradient is very small. In other words, structural steels with a BCC crystal structure undergo equiaxed dendrite coagulation. However, in structural steels with an FCC crystal structure, such as in austenitic stainless steel, subgrain boundaries are easily observed even at room temperature because diffusion at high temperature is relatively slow. The finer the grain, the more improved is its hardness and toughness characteristics.

3.2. Hardness

The hardness at the cross section of the base material removed after installation of the lifting lug of low grade steel was measured. The hardness measurement position is 2 mm in the thickness direction from the surface as shown in Fig. 9 (a) and the steel surface with the lugs removed as shown in Fig. 9 (b). Hardness was measured at intervals of 0.5 mm 10 (a) is the results at 2 mm away from the surface in the thickness direction, and Fig. 10 (b) is the result at the surface with the lugs removed.

The hardness values in the base metal section varied depending on its type. EH36 steel had a hardness value of 20–40 Hv more than the B-grade steel. In the results obtained, large hardness values were observed near the welds. Particularly, the hardness value on the cross section of F4 was 100–150 Hv more than those on the cross sections of F1, F2, and F3, while the hardness values on the

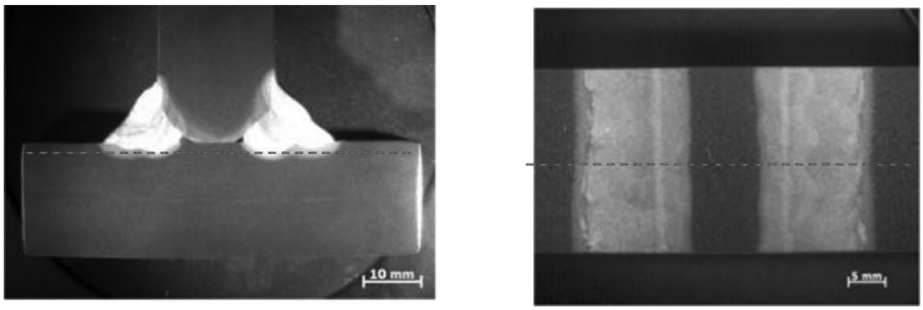

Fig. 9. Position of hardness in F1.

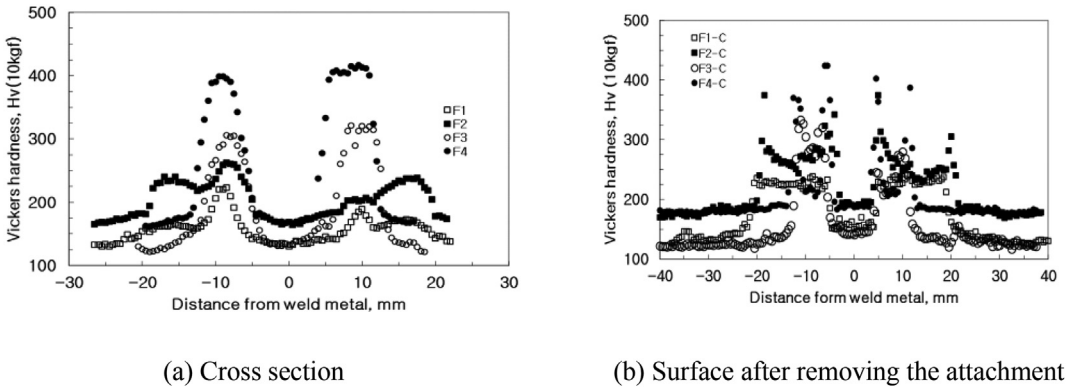

(a) Cross section (b) Surface after removing the attachment

Fig. 10. Hardness Micro structure.

surfaces of F3 and F4 were 100 Hv more than those on the surfaces of F1 and F2. The maximum hardness value was found to be larger than the standard value of 380 Hv. This high hardness value was not due to the use of a dissimilar lug but because of differences in the cooling rate, i.e., an inappropriate welding procedure. Adams (1958) reported that the cooling rate of a weld depends on the thickness of the weld, shape of the weld, temperature of the base metal, heat input to the weld, and preheat temperature. The austenite microstructure formed by high temperatures of welding shows various phase changes depending on the cooling rate. When the critical cooling rate is high, all the microstructures are transformed into martensites. However, when the critical cooling rate is low, bainite and pearlite transformations occur, and the hardness value subsequently decreases. According to the Hall-Petch equation (Park et al. (2003)), the finer the particle size, the better the hardness and toughness performance. The heat inputs of specimens F1 and F2 are higher than those to F3 and F4 because specimens F1 and F2 have a groove welding and the thickness (10 mm) of F3 and F4 is thinner and are fillet welded with a throat length of 4 mm; hence, the cooling rates of specimens F3 and F4 were faster than those of

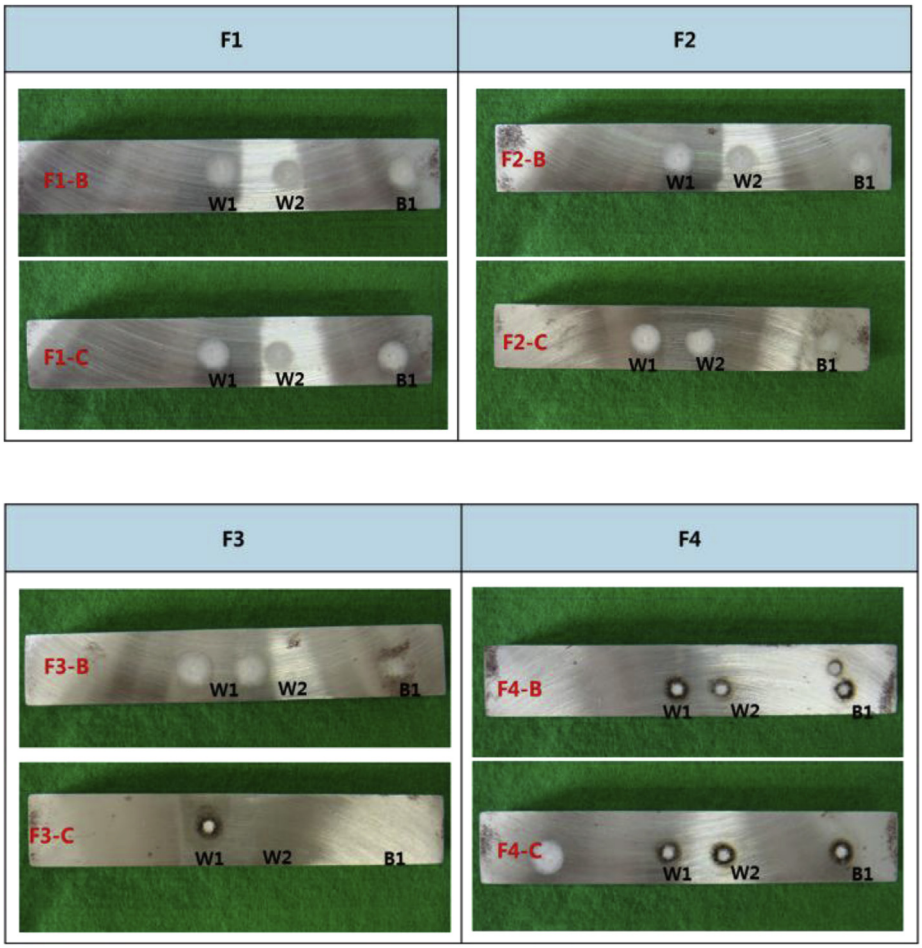

Fig. 11. Position of dilution test for fillet welding joint.

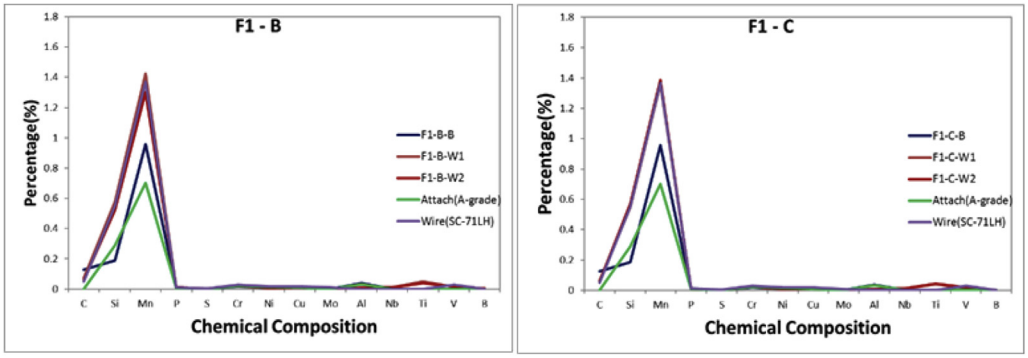

(a) Specimen F1

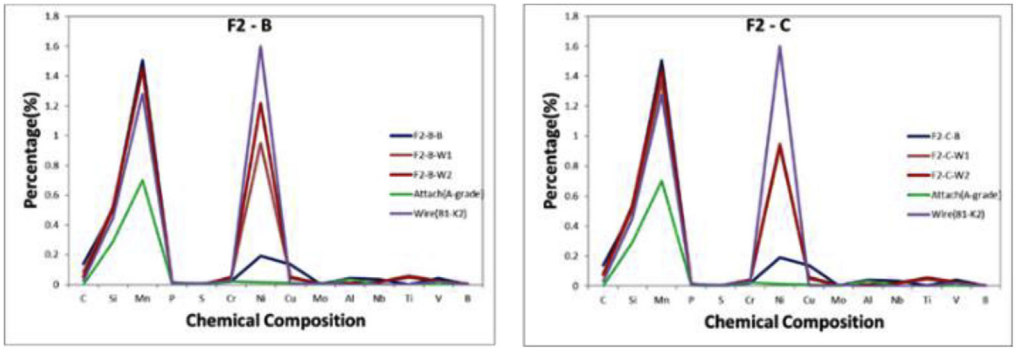

(b) Specimen F2

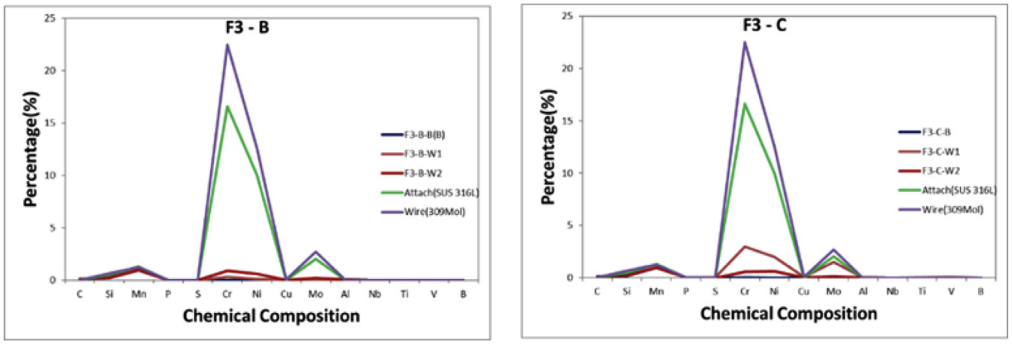

(c) Specimen F3

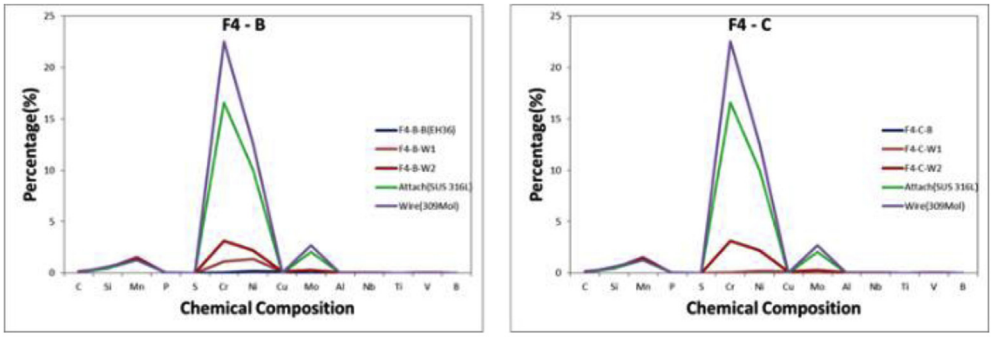

(d) Specimen F4

Fig. 12. Results of chemical composition analysis for removal attached plate in fillet joint.

F1 and F2. Consequently, F4 had the fastest cooling rate and subsequently the largest hardness value.

3.3. Metal element component analysis

Emission spectrochemical analysis was performed to examine whether the metal component of the lug was transferred to the base metal and diluted during the lifting-lug welding process. This analysis is a method of quantitatively analyzing spectral intensity at the wavelength of light generated by irradiating a sample and determining the type or amount of component element of the sample based on the emission spectrum of a standard reference sample. Fig. 11 is an image of the component analysis of the surface from where the lugs were removed. The measurement positions were fixed at locations W1 and W2 at the center of the welding length and boxing welded joint, respectively. The component analysis of the lug, base metal, and welding wire were compared with the spectral analysis results of the measured surfaces W1 and W2.

Fig. 12 shows a comparison of the components detected at the two measured locations (W1, W2) with those detected in the base metal (B), welding wire (Wire), and attached metal (Attach). The results of F1 in Fig. 12(a) show that about 0.2–0.4% of Si and 1.4% of Mn was detected at W1 and W2 and in the welding wire, respectively. In the lag material, Mn was detected in 0.6–0.7% and 1% in the base material. From these results, the locations (W1, W2) of F1 were concluded similar to the welding wire. However, the lug component was not detected. The results of F2 in Fig. 12(b) show that about 0.6% of Si, 1.5% of Mn, and 1% of Ni were detected at W1, W2, and in the welding wires. In the lag material, Mn was 0.6–0.7%, while in the base metal, Si and Mn were the same as those measured in W1 and W2, and 0.1% Ni was detected. From these results, the chemical composition of the position (W1, W2) of F2 was detected similar to welding wire and base metal, but no component of lag metal was detected. The results of F3 and F4, shown in Fig. 12(c) and (d), respectively, are similar. In the welding wire and at W1 and W2, the amount of Mn detected was within 1% and the amounts of Cr and Ni were within 4%. The chemical composition of the base metal was found to be similar to that of the locations W1 and W2. The welding wire and lug were found to contain 15–22% of Cr and Mn and about 3% of Mo.

The results confirmed that the chemical composition of the locations W1 and W2 was similar to those of the base metal and welding wire and not to that of the lug metal. The results also confirmed that this similarity depends on the degree of removal of the weld bead. Moreover, the results at the surface from where the lug was removed also confirmed the absence of the chemical composition of the lug metal.

4. Conclusions

To investigate the effect of the removal of lifting lug on the physical properties of the base metal, the microstructures, hardness, and chemical composition of the base metal were compared to those of the lug metal, and the following results were obtained:

1. After removing the lugs, all the metal microstructures of the test specimens melded with and appeared as the metal microstructures of the welding wire itself, and the lugs did not demonstrate any effect. In the case of the base metal, the EH36 shipbuilding steel showed a better microstructure than the B-grade steel. The microstructure of EH36 steel was also visible in the fusion line near the weld.
2. The hardness values measured after the removal of the lugs were larger in F3 and F4 specimens than in F1 and F2 specimens. Particularly, the result of F4 exceeded 380 Hv locally. This is because F3 and F4 received smaller amounts of heat inputs than F1 and F2. Moreover, the test specimen F4 showed a high hardness value because the thickness of its base metal was 30 mm, which is thicker than those of the other specimens. Hence, the cooling rate at the welded portion of F4 was the fastest.
3. Analysis of the chemical composition of the section from where the lug was removed revealed that the lug component diluted and appeared as a component of the welding wire or the base metal. This is because the welding wire melted and penetrated into the base metal, as evident from the cross-section of the welding joint.
4. After analyzing the metal microstructure, hardness value, and chemical composition after the removal of the lugs, most of the properties of the welding wire and base metal persisted, and the lug did not have any influence on the physical properties of the base metal.

Acknowledgments

This research was supported by Basic Science Research Program through the National Research Foundation of Korea (NRF) funded by the Ministry of Education (NRF-2016R1D1A1B01014412).

References

Adams, 1958. Colling rates and peak temperatures in fusion welding. Weld. J. Res. 210~215 supplement.

An, Gyubaek, Hong, Seunglae, Park, Jeongung, Ro, Chanseung, Han, Ilwook, 2017. Identification of correlation between fracture toughness parameters of cryogenic steel weld joints. J. Weld. Join. 35 (3), 82–87. https://doi.org/10.5781/JWJ.2017.35.3.12.

American Society of Mechanical Engineers (ASME), 2008. ASME-BTH–1; Design of Below-The-Hook Lifting Devices. ASME, USA.

Gunaraj, V., Murugan, N., 1999. Prediction and comparison of the area of the heat-affected zone for the bead-on-plate and bead-on-joint in submerged arc welding of pipes. J. Mater. Process. Technol. 95 (1–3), 246–261. https://doi.org/10.1016/S0924-0136(99)00296-4.

Ham, Juh-Hyeok, 2001. Development of the design system for the lifting lug structure. J. Soc. Naval Architect. Korea 38 (1), 86–98.

Ham, Juh-Hyeok, 2011. Parametric design considerations for lifting Lug structure on ship block. J. Ocean Eng. Technol. 25 (2), 101–107.

Ham, Juh-Hyeok, Kim, Dong-Jin, 2009. Consideration of the lifting lug structure using the hybrid structural design system. J. Ocean Eng. Technol. 23 (2), 104–109.

Hoshino, Manabu, Saitoh, Naoki, Muraoka, Hirohide, Saeki, Osamu, 2004. Development of super-9%Ni steel plates with superior low-temperature toughness for LNG storage tanks. Nippon Steel Tech. Rep. 90, 20–24.

Kim, Sang-il, 2003. Design for raising the rate of recovering use of lifting lug. J. Soc. Naval Architect. Korea 40 (4), 59–65.

Kim, Sang-il, 2006. Block lifting analysis to examine the cause of cracking in the hopper top plate. J. Ocean Eng. Technol. 20 (1), 16–19.

Kim, Oi-Hyun, Kim, Jeong-Je, 1998. Reliability assessment of ship longitudinal strength for the rational ship structural design. J. Ocean Eng. Technol. 12 (4), 8–15.

Kim, Gwang-Soo, Kim, Dae-Sun, Choi, Young-Ki, 1996. Study on the formation and prevention of weld defect on the surface ground after removing the weld for lifting lug. In: Summer Conference of the Korean Welding and Joining Society 1996.

Nouri, M., Abdollah-zadehy, A., Malek, F., 2007. Effect of welding parameters on dilution and weld bead geometry in cladding. J. Mater. Sci. Technol. 23 (6), 817–822.

Om, Hari, Pandey, Sunil, 2013. Effect of heat input on dilution and heat affected zone in submerged arc welding process. Sadhaba _Acad. Proc. Eng. Sci. 38 (6), 1369–1391.

Park, Seung Hwan C., Sato, Yutaka S., Kokawa, Hiroyuki, 2003. Microstructural evolution and its effect on Hall-Petch relationship in friction stir welding of thixomolded Mg alloy AZ91D. J. Mater. Sci. 38 (21), 4379–4383.

Welding handbook (8th), 1991. American Welding Society, vol. 1, pp. 95–100.